Flow induced rigidity percolation in shear thickening suspensions

Abhay Goyal and Nicos S. Martys
Infrastructure Materials Group, Engineering Laboratory, National Institute of Standards and Technology,

Emanuela Del Gado
Dept of Physics, Institute of Soft Matter Synthesis and Metrology, Georgetown University, Washington DC, USA

Discontinuous shear thickening (DST) is associated with a sharp rise of a suspension's viscosity with increasing applied shear rate. A key signature of DST, highlighted in recent studies, is the very large fluctuations of the measured stress as the suspension thickens. A clear link between microstructural development and the dramatic increase of the stress fluctuations has not been established yet. To identify the microstructural underpinnings of this behavior, we perform simulations of sheared dense suspensions. By analyzing particle contact networks, we identify a subset of constrained particles that contribute directly to the rapid rise in viscosity and the large stress fluctuations. Indeed, both phenomena can be explained by the growth and percolation of constrained particle networks—in direct analogy to rigidity percolation. A finite size scaling analysis confirms this is a percolation phenomenon and allows us to estimate the critical exponents. Our findings reveal the specific microstructural transition that underlies DST.

Suspensions play an important role in a wide variety of environmental and technological processes. Examples include colloidal systems, pharmaceuticals, slurries, and concrete. Their flows raise a number of fundamental physics questions, exhibiting a multitude of phenomena that include shear thinning and thickening, thixotropy, giant stress fluctuations and jamming [1, 2]. While several problems remain outstanding, intense interest has focused on the physical mechanisms at the origin of the discontinuous shear thickening (DST), which is quite ubiquitous and dramatic: the suspension experiences a rapid rise in stress or viscosity as the imposed shear rate increases. The flow of DST suspensions rapidly becomes strongly dilatant [3–5] and erratic, with giant stress fluctuations, rapid increase of stress, and structural inhomogeneities in response to the increasing shear rate [6–9].

Recent studies on DST have gained new insights into the role of frictional solid-on-solid contacts between the particles in a suspension, and how their sharp increase in number largely controls the emergence of DST [10–13]. Indeed, over the last few years, experiments and numerical simulations have extensively analyzed and demonstrated, how, at the onset of DST, the bulk rheological behavior of suspensions becomes dramatically sensitive to the surface interactions, roughness, and hence frictional contact between particles, in spite of the presence of solvent lubrication forces [5, 14–20]. This fundamental understanding of such phenomena has opened new paths to design the flow of dense suspensions through nanoscale physics and surface chemistry. However, in spite of the sensitivity to particle surface contacts which are strongly material and chemistry dependent, the overall DST phenomenology is consistent across the whole spectrum of suspensions involved, suggesting the presence of common microstructural features which remain elusive.

The theoretical mean-field approach of Wyart and Cates [12], in which the microstructure is characterized by the suspension volume fraction and the overall fraction of frictional contacts produced under shear, demonstrated that the sudden rise in the stress (or decrease in shear rate for the case of stress driven shear) has general features that do not depend on the specifics of the material and surface chemistry. Further, the large fluctuations of the shear stresses and the scaling properties of the shear response, which are reminiscent of critical phenomena, seem ubiquitous in DST over a wide range of suspensions [7–9, 21, 22].

These findings suggest that, as frictional contacts between the particles become prevalent with increasing rate, larger scale microstructures, involving many particles and built under shear, may emerge independently from the detailed material chemistry and control the DST phenomenon [23]. Previous studies have focused on order-disorder transitions in the microstructure of particle suspensions approaching shear thickening [24–26], and there is now growing consensus, from experiments and simulations, that large clusters or chains of particles spanning the system may cause the abrupt increase of stress or possibly jamming [10, 12, 27–30]. Clearly, the fact that there is microstructural reorganization that eventually spans the system is suggestive of a percolation transition [31, 32]. The occurrence of a percolation transition could provide a connection to critical phenomena [31], and could provide a conceptual framework for understanding aspects of both the microstructural development and its link to DST. However, testing these ideas is extremely challenging, since microstructures, and in particular stress-bearing ones, are hardly accessible in experiments on dense suspensions subjected to high shear stresses or rates. Computer simulations of particle based models may instead be specifically designed to investigate those microstructures, and are therefore the most promising tool to shed light onto these questions. Nevertheless, due to their complexity, most simulations studies have been so far limited to relatively small system sizes,

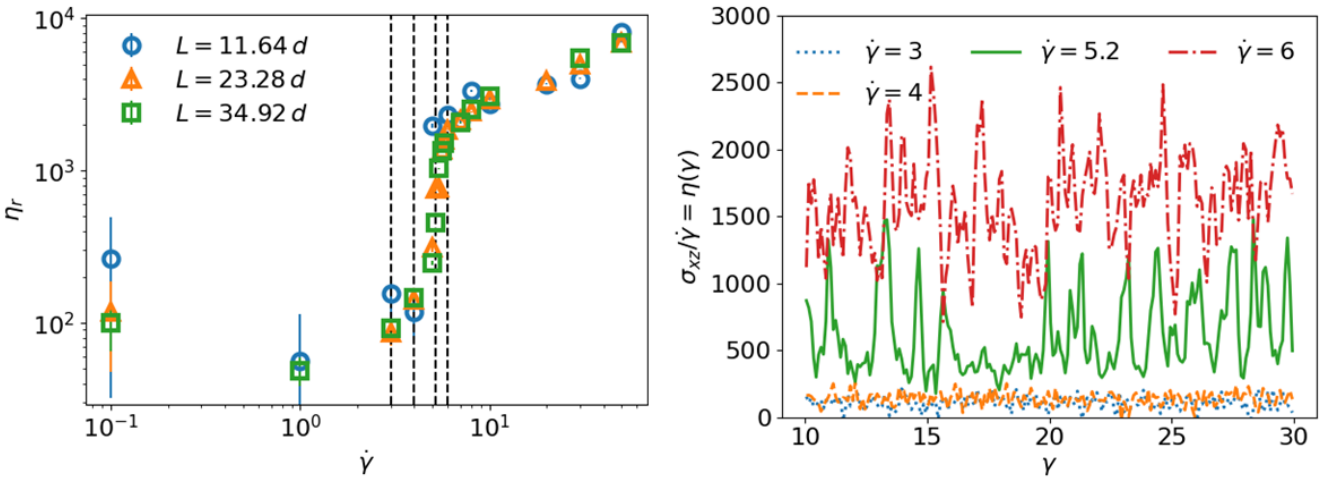

FIG. 1: **(a)** The average relative viscosity (η_r) as a function of shear rate ($\dot{\gamma}$) for a suspension at $\phi = 56$ % and different system sizes. The error bars represent one standard deviation from the mean that was calculated, after a dynamical equilibrium was reached, from a running average over 25 strain units. The jump in the viscosity does not vary with increasing the system nor the Reynolds number (albeit reducing the Reynolds number produces a plateau at very high rates). The vertical dashed lines indicate the shear rates used in **(b)**, where we show the instantaneous viscosity (stress/shear rate) as a function of applied strain γ. The jump in η_r is accompanied by large fluctuations of the stress near the critical shear rate.

whereas much larger system sizes would be needed to detect critical-like behaviors, and identify their origin.

Here we use large scale 3D simulations of model dense suspensions to show that a percolation transition is indeed at the origin of the stress fluctuations characteristic of DST, once one properly defines the basic unit of microstructure that forms the percolating structure. The percolation of this microstructure can be directly linked to the DST, and to the accompanying large stress fluctuations, and points to the role of rigidity percolation in this phenomenon. Further, the critical behavior is studied by applying a finite size scaling analysis, which allows us to estimate the related critical exponents.

We have utilized computer simulations to study a model suspension of spheres that interact via hydrodynamic lubrication, contact repulsion, and frictional forces, following recent work on simulations of shear thickening suspensions [26, 33, 34]. All spheres have the same size, while all interaction parameters, provided in the supplementary information (SI), have been adjusted to match the model in [34] where lubrication forces are regularized at short distances between the particles surfaces and Coulomb friction act tangentially on surface contacts. We follow the same numerical approach described in [26] to integrate the equations of motion for all particles, which allows us to perform simulations of large systems with LAMMPS [35] with overdamped particle motions. The system is sheared using Lees-Edwards boundary conditions, and a background velocity field with constant shear rate is imposed that particle motion can relax to. The system is also subject to thermal fluctuations. All quantities are reported in reduced units as a combination of three basic units: energy scale $\varepsilon = k_B T$, particle mass m, and particle diameter d. From these parameters, the unit of time is $\tau_0 = \sqrt{md^2/\varepsilon}$. Here we present data on volume fraction $\phi = 56\,\%$, and we reproduce, as in [34], the features of the DST. The data reported in the following refer to simulation boxes with edge length, L= 11.64 d, 23.28 d and 34.92 d, containing 1688, 13500 and 45563 spheres respectively. The medium and larger sizes correspond to much larger system sizes than previous studies, which is essential to address the critical-like behavior of stress fluctuations and to deal with finite-size effects. We use the convention that x corresponds to the flow direction, y corresponds to the vorticity direction, and z to the shear gradient direction. The model suspensions were sheared up to 40 strain units to reach a steady flow state. We use the shear component σ_{xz} of the stress tensor, obtained from interparticle forces, relative positions, and particle velocities [36], to extract the relative viscosity η_r which is plotted in Figure 1a as a function of the shear rate $\dot{\gamma}$ for the three system sizes studied. The data show a steep increase of viscosity at a threshold shear rate $\dot{\gamma} \simeq 5\ {\tau_0}^{-1}$, and increasing the system size does not significantly alter the viscosity increase, indicating that the DST phenomenon identified here is not an artifact of limited sample sizes used in simulations. The time series from which the viscosity is extracted in steady state are plotted in Figure 1b, which shows (for the intermediate system size of 13500 particles) $\sigma_{xz}/\dot{\gamma}$ as a function of the strain γ for several shear rates. The data clearly demonstrate the presence of large fluctuations of the shear stress in systems that have gone through DST.

As described earlier, the number of frictional contacts per particle is strongly correlated to the suspension stress close to shear thickening. Recent work [32] has shown that the shear stress increases with the mean frictional

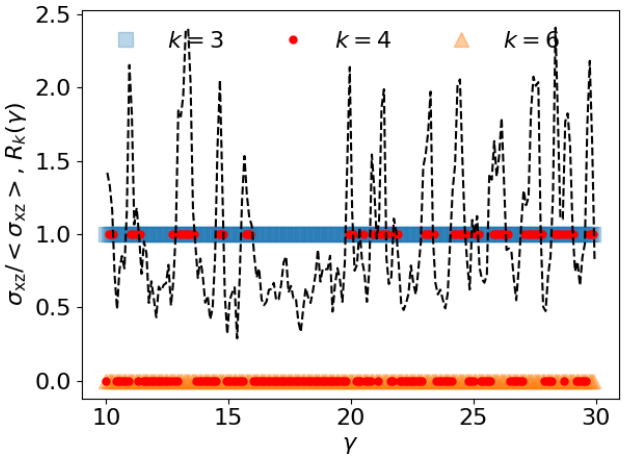

FIG. 2: $R_k(\gamma)$ (equal to 1 if there exists at a percolating cluster of k-neighbor particles and 0 otherwise) plotted for different k values alongside the stress $\sigma_{xz}/ < \sigma_{xz} >$ (dashed black line). The percolation of 4-neighbor particles corresponds to the giant stress fluctuations.

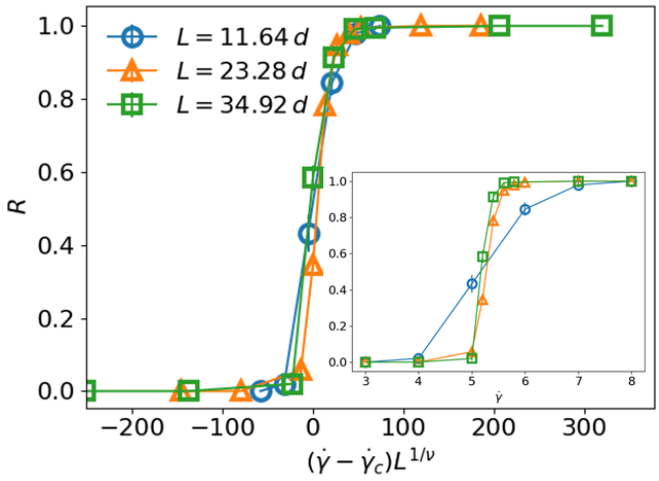

FIG. 3: Main frame: The probability R of 4-neighbor particles to form a percolating cluster as a function of the scaling variable $(\dot{\gamma}-\dot{\gamma}_c)L^{1/\nu}$ for three system sizes. The data collapse onto a unique curve for $\dot{\gamma}_c = 5.2\tau_0^{-1}$ and $\nu \approx 0.6$. Inset: The probability R of 4-neighbor particles to form a percolating cluster as a funtion of the shear rate for the different system sizes.

contact number, peaking at 3 and 4 for large shear rates. However, in terms of the mean frictional contact number, a distinction could not be made between continuous shear thickening (CST) and DST, which clearly have different rheological signatures. These findings point, in our view, to the fact that the local microstructural environment and its larger scale connectivity determines the nature of the stress transmission through the particle suspension. As a consequence, to search for the microscopic origin of the stress fluctuations, we consider the hierarchy of structures built up by particles that share frictional contacts with a minimum k neighbors. In graph theory this defines a contact graph (also called a network) composed of nodes with degree k at minimum [37, 38]. To be more precise, we define a neighbor, for each particle, as a particle close enough in proximity that it can interact with said particle by frictional forces. In our frictional model, this occurs when the sphere surfaces are in contact. The frictional force is proportional to the normal force between the neighboring spheres and acts to resist transverse motion relative to surface normal between neighboring spheres (see SI). We will refer to particles with at least k neighbors as k-neighbor particles.

Testing k values from 2 to 6, we determine whether the percolation of k-neighbor particles can be directly connected to the rapid rise in viscosity and the large stress fluctuations corresponding to the DST in our simulations. For each k, we identify the k-neighbor particles, sort them into clusters, obtain the cluster size distribution, and identify configurations in which at least one percolating cluster is present in all directions. The plot in Figure 2 superimposes the time series for the presence of a percolating cluster of k-neighbor particles ($R_k = 1$) or not ($R_k = 0$), for different k, to the time series of the shear stress close to DST. The data show that clusters of 3-neighbor particles always percolate, independently from the stress fluctuations, which also happens for k=2 (data not shown). In contrast, the percolation of a 4-neighbor cluster exactly corresponds to the spikes in the shear stress of the suspension. Note, the 4-neighbor particles locally satisfies the Maxwell criterion for rigidity in presence of tangential frictional forces [39]. We also find that at low enough $\dot{\gamma}$, where DST does not occur and stress fluctuations are much smaller, the percolation of 4-neighbor particles were not observed. At higher k values, percolation is significantly reduced [32]. Indeed, the data in Figure 2 show that percolation of 6-neighbor particles, which, incidentally, correspond to locally rigid structures for frictionless spheres, is not evident.

These findings strongly suggest that the percolation of locally rigid structures, reminiscent of shear jamming in granular fluids [40, 41], may be at the origin of the large stress fluctuations typical of DST, playing a significant role in this phenomenon. Indeed, the percolation of the rigid 4-neighbor particles can support the transmission of stress and bear most of the load also over an extended period of time, in contrast to k-neighbor particles with k lower values, which can more easily be disrupted. The percolation of the rigid 4-neighbor particles may therefore be central to the self-organization of the microstructure of the suspensions under flow, when DST occurs.

It is intriguing, at this point, to ask whether the growth of 4-neighbor particles can be studied in terms of percolation theory. That is, can we define a critical shear rate and critical exponents that describe a diverging length scale and mean cluster size? The determination of such quantities can be challenging even for static systems.

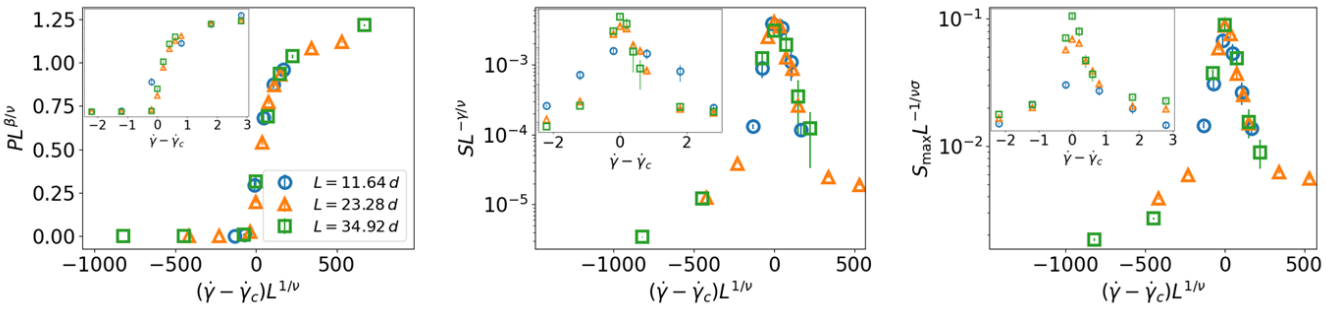

FIG. 4: Left: $PL^{\beta/\nu}$, with P the probability of a random 4-neighbor particle to belong to the percolating cluster, as a function of the scaling variable $(\dot\gamma-\dot\gamma_c)L^{1/\nu}$ and for different system sizes. Center: $SL^{-\gamma/\nu}$, with S the second moment of the cluster size distribution (or mean cluster size), as a function of $(\dot\gamma-\dot\gamma_c)L^{1/\nu}$. Right: $S_{\max}L^{-1/\nu\sigma}$, with $S_{\max}$ the maximum cluster size, as a function of $(\dot\gamma-\dot\gamma_c)L^{1/\nu}$ and for different system sizes. Using $\dot\gamma_c = 5.1\tau_0^{-1}$ obtained from the percolation probability (see Fig.3), all data collapse onto unique scaling curves for $\beta \approx 0.18$, $\sigma \approx 0.75$, and $\gamma \approx 1.3$. Insets: Unscaled P (left), S (center), and $S_{\max}$ (right) plotted against $\dot\gamma$ for the different system sizes.

Here we use a finite size scaling ansatz typical of critical phenomena and percolation [31] to first determine the critical shear rate. We examine the probability of percolation, R, defined as the average occurrence of percolating clusters of 4-neighbor particles over each time series at different shear rates and for the 3 different sizes of the simulation box. The data for R as a function of shear rate (Figure 3 inset) show that the larger the system size the steeper the transition from 0 to 1 in probability, akin to the behavior of the percolation probability close to a percolation transition, and that the curves for each system size intersect at around a shear rate of about 5. Hence we hypothesize that the percolation threshold of the 4-neighbor particles indeed corresponds to a specific shear rate. By defining the approximate intersection of the different curves as the critical shear rate corresponding to the percolation threshold, we can collapse all data in terms of a scaling variable $(\dot\gamma-\dot\gamma_c)L^{1/\nu}$. γ_c points to a characteristic time scale over which a stable percolating network may be built or destroyed at a given shear rate (Figure 3). In general, we would expect that, quantitatively, this characteristic timescale depends on the microscopic physics of the system, and hence on the specific experimental system considered or on the microscopic parameters of the simulations (see SI).

The data collapse supports the validity of the finite size scaling ansatz and provides a first estimate for the critical exponent ν, $\nu \approx 0.6$, which describes the divergence of the correlation length close to the percolation threshold. We can then compute, from the same cluster analysis of 4-neighbor particles and having obtained the whole cluster size distribution, the probability of a k-neighbor random particle being in the percolating cluster, the mean cluster size (i.e. the second moment of the cluster size distribution), and the maximum cluster size [31]. All these quantities follow the data collapse which stems from the finite size scaling ansatz (Figure 4), and the collapsed data allow us to independently determine three different critical exponents: $\beta \approx 0.18$, $\sigma \approx 0.75$, and $\gamma \approx 1.3$. The exact determination of the critical exponents will require further studies, however, the data already show a significant discrepancy from the mean field values and from the random connectivity percolation transition in $3D$, suggesting that the percolation of the 4-neighbor particles during DST may correspond to a distinct universality class. Rigidity percolation studies, while quite limited (especially in $3D$), have indeed suggested a distinct universality class, and frictional rigidity percolation studies have found similar discrepancies [39, 42].

In conclusion, we have identified the basic microstructural unit whose percolation corresponds to the onset of DST in shear thickening suspensions, thanks to large scale 3D simulations of model suspensions. Remarkably, these microstructural units can build a locally rigid network of frictional contacts and their cluster statistics follow the finite size scaling ansatz typical of critical phenomena and percolation theory. The percolation of these locally rigid structures is central in the stress transmission throughout the suspension and appears be at the origin of the giant fluctuations and the critical-like behaviors observed for DST. The snapshots in Figure 5 indeed show how the rigid structures identified through the 4-neighbor particles change drastically with the global stress measured in the system, providing a visualization of the microstructural origin of the giant stress fluctuations.

As our findings support the idea that a very specific self-organization of the suspension microstructure has to take place during DST, they call on experimental approaches that can recognize the locally rigid structures. For example, efforts in the past to study the conductivity of a suspension of particles, where the matrix fluid is conducting and the spherical particles are insulating, can distinguish between ordered and disordered states [43]. However, this is not sufficient to distinguish be-

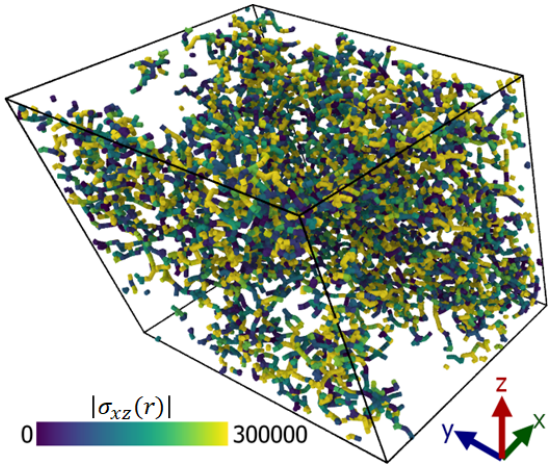

FIG. 5: A snapshot showing the connections between 4-neighbor particles at $\dot{\gamma} = 5\,\tau_0^{-1}$. The connections are colored by the magnitude of the local shear stress, $|\sigma_{xz}|$. In this snapshot, $\sigma_{xz} \approx 4000\,k_BT/d^3$, which is accompanied by the presence a large number of 4-neighbor particles and their percolation. Here we show only the percolating cluster, corresponding to roughly half of the 4-neighbor particles present, which forms a densely connected network that spans the system in all directions. See Supplementary Material for a snapshot from the low-stress state.

tween different k-neighbor particles, making it a challenge to identify the type of structure which is percolating. Experiments that can image stress fields [9, 44, 45] will likely pick out stress chains in compression. This is not necessarily enough to directly identify the 4-neighbor particle network which appears to be crucial for DST, although the stability of a percolating stress chain may indicate it follows a connected path of $k = 2$ neighbor particles which would be a subset of a network of $k = 4$ neighbor particles, providing the necessary structure to support stress chains. Developing capability to identify the mechanical constraints acting locally on particles in different part of the suspension contact network may be central to test the insight gained in this work. As extensive large scale simulations could allow, in the future, to more precisely determine the universality class from the percolation exponents, experimental rheological tests and scaling analysis of experimental flow curves [18, 22, 30] could complement the microscopic understanding developed here. Following the hierarchical self-organization of the k-neighbor particle structures under shear and identifying possible precursors of the rigidity percolation could also provide novel insight into shear thickening instabilities.

Acknowledgements. The authors acknowledge the NIST PREP Gaithersburg Program (70NANB18H151) and National Science Foundation (NSF DMR-2026842).

[1] E. Guazzelli and J. F. Morris, *A Physical Introduction to Suspension Dynamics* (Cambridge University Press, 2012).
[2] J. Mewis and N. J. Wagner, *Colloidal Suspension Rheology* (Cambridge University Press, 2011).
[3] R. L. Hoffman, Transactions of the Society of Rheology **16**, 155 (1972).
[4] D. Leighton and A. Acrivos, Journal of Fluid Mechanics **181**, 415–439 (1987).
[5] J. R. Royer, D. L. Blair, and S. D. Hudson, Physical Review Letters **116**, 1 (2016), ISSN 10797114, 1603.00422.
[6] D. Lootens, H. Van Damme, and P. Hébraud, Phys. Rev. Lett. **90**, 178301 (2003), URL `https://link.aps.org/doi/10.1103/PhysRevLett.90.178301`.
[7] M. Hermes, B. M. Guy, W. C. K. Poon, G. Poy, M. E. Cates, and M. Wyart, Journal of Rheology **60**, 905 (2016).
[8] B. Saint-Michel, T. Gibaud, and S. Manneville, Phys. Rev. X **8**, 031006 (2018), URL `https://link.aps.org/doi/10.1103/PhysRevX.8.031006`.
[9] V. Rathee, D. L. Blair, and J. S. Urbach, Proceedings of the National Academy of Sciences **114**, 8740 (2017), https://www.pnas.org/doi/pdf/10.1073/pnas.1703871114, URL `https://www.pnas.org/doi/abs/10.1073/pnas.1703871114`.
[10] R. Seto, R. Mari, J. F. Morris, and M. M. Denn, Physical Review Letters **111**, 1 (2013), ISSN 00319007, 1306.5985.
[11] R. Mari, R. Seto, J. F. Morris, and M. M. Denn, Journal of Rheology **58**, 1693 (2014), ISSN 0148-6055, 1403.6793, URL `http://dx.doi.org/10.1122/1.4890747`.
[12] M. Wyart and M. E. Cates, Physical Review Letters **112**, 1 (2014), ISSN 10797114, 1311.4099.
[13] N. Y. C. Lin, B. M. Guy, M. Hermes, C. Ness, J. Sun, W. C. K. Poon, and I. Cohen, Phys. Rev. Lett. **115**, 228304 (2015), URL `https://link.aps.org/doi/10.1103/PhysRevLett.115.228304`.
[14] D. Lootens, P. Hébraud, E. Lécolier, and H. Van Damme, Oil and Gas Science and Technology **59**, 31 (2004), ISSN 12944475.
[15] J. F. Morris, Phys. Rev. Fluids **3**, 110508 (2018), URL `https://link.aps.org/doi/10.1103/PhysRevFluids.3.110508`.
[16] S. Jamali and J. F. Brady, Physical Review Letters **123**, 138002 (2019), ISSN 10797114, URL `https://doi.org/10.1103/PhysRevLett.123.138002`.
[17] M. Wang, S. Jamali, and J. F. Brady, Journal of Rheology **64**, 379 (2020), ISSN 0148-6055.
[18] E. Y. X. Ong, M. Ramaswamy, R. Niu, N. Y. C. Lin, A. Shetty, R. N. Zia, G. H. McKinley, and I. Cohen, Journal of Rheology **64**, 343 (2020), ISSN 0148-6055.
[19] R. V. More and A. M. Ardekani, Journal of Rheology **64**, 67 (2020), ISSN 0148-6055.
[20] M. Nabizadeh, A. Singh, and S. Jamali, Phys. Rev. Lett. **129**, 068001 (2022), URL `https://link.aps.org/doi/10.1103/PhysRevLett.129.068001`.
[21] O. Sedes, A. Singh, and J. F. Morris, Journal of Rheology **64**, 309 (2020), https://doi.org/10.1122/1.5131740, URL `https://doi.org/10.1122/1.5131740`.
[22] M. Ramaswamy, I. Griniasty, D. B. Liarte, A. Shetty, E. Katifori, E. Del Gado, J. P. Sethna, B. Chakraborty,

and I. Cohen (2021), 2107.13338, URL http://arxiv.org/abs/2107.13338.

[23] R. Seto, A. Singh, B. Chakraborty, M. M. Denn, and J. F. Morris, Granular Matter **21**, 1 (2019), ISSN 14347636, 1902.04361, URL https://doi.org/10.1007/s10035-019-0931-5.

[24] J. Bender and N. J. Wagner, Journal of Rheology **40**, 899 (1996), ISSN 0148-6055.

[25] S. D. Kulkarni and J. F. Morris, Journal of Rheology **53**, 417 (2009), ISSN 0148-6055.

[26] A. Goyal, E. Del Gado, S. Z. Jones, and N. S. Martys, Journal of Rheology **66**, 1055 (2022), https://doi.org/10.1122/8.0000453, URL https://doi.org/10.1122/8.0000453.

[27] J. E. Thomas, K. Ramola, A. Singh, R. Mari, J. F. Morris, and B. Chakraborty, Phys. Rev. Lett. **121**, 128002 (2018), URL https://link.aps.org/doi/10.1103/PhysRevLett.121.128002.

[28] L. E. Edens, E. G. Alvarado, A. Singh, J. F. Morris, G. K. Schenter, J. Chun, and A. E. Clark, Soft Matter **17**, 7476 (2021), ISSN 17446848.

[29] M. Gameiro, A. Singh, L. Kondic, K. Mischaikow, and J. F. Morris, Phys. Rev. Fluids **5**, 034307 (2020), URL https://link.aps.org/doi/10.1103/PhysRevFluids.5.034307.

[30] N. Y. C. Lin, C. Ness, M. E. Cates, J. Sun, and I. Cohen, PNAS **113**, 10774 (2016).

[31] D. Stauffer and A. Aharony, *Introduction to Percolation Theory* (CRC Press, 2018), ISBN 9781315274386.

[32] O. Sedes, H. A. Makse, B. Chakraborty, and J. F. Morris, Phys. Rev. Fluids **7**, 024304 (2022), URL https://link.aps.org/doi/10.1103/PhysRevFluids.7.024304.

[33] R. Mari, R. Seto, J. F. Morris, and M. M. Denn, Proceedings of the National Academy of Sciences of the United States of America **112**, 15326 (2015), ISSN 10916490, 1508.01243.

[34] A. Singh, R. Mari, M. M. Denn, and J. F. Morris, Journal of Rheology **62**, 457 (2018), ISSN 0148-6055, 1708.05749, URL http://dx.doi.org/10.1122/1.4999237.

[35] S. Plimpton, Journal of Computational Physics **117**, 1 (1995), ISSN 00219991, nag.2347, URL http://lammps.sandia.gov.

[36] R. Evans, Journal of Physics: Condensed Matter **2**, 8989 (1990), ISSN 09538984.

[37] F. Morone, K. Burleson-Lesser, H. Vinutha, S. Sastry, and H. A. Makse, Physica A: Statistical Mechanics and its Applications **516**, 172 (2019), ISSN 0378-4371, URL https://www.sciencedirect.com/science/article/pii/S0378437118313839.

[38] A. Papadopoulos, M. A. Porter, K. E. Daniels, and D. S. Bassett, J. Complex Netw. **6**, 485 (2018).

[39] K. Liu, S. Henkes, and J. M. Schwarz, Phys. Rev. X **9**, 021006 (2019), URL https://link.aps.org/doi/10.1103/PhysRevX.9.021006.

[40] B. Dapeng, J. Zhang, B. Chakraborty, and R. P. Behringer, Nature **480**, 355 (2011).

[41] H. A. Vinutha and S. Sastry, Nature Physics **12**, 578 (2016), ISSN 17452481, 1510.00962.

[42] D. J. Jacobs and M. F. Thorpe, Phys. Rev. E **53**, 3682 (1996), URL https://link.aps.org/doi/10.1103/PhysRevE.53.3682.

[43] P. Hébraud, private communication.

[44] I. Jorjadze, L.-L. Pontani, and J. Brujic, Phys. Rev. Lett. **110**, 048302 (2013), URL https://link.aps.org/doi/10.1103/PhysRevLett.110.048302.

[45] N. Y. C. Lin and I. Cohen, Soft Matter **12**, 9058 (2016), URL http://dx.doi.org/10.1039/C6SM02079H.